Quaternary International 436 (2017) 173–180

Contents lists available at ScienceDirect

Quaternary International

journal homepage: www.elsevier.com/locate/quaint

Potential degradation effect on paleo-moisture proxies based on the relative abundance of archaeal vs. bacterial tetraethers in loess-paleosol sequences on the Chinese Loess Plateau

Huanye Wang [a, *], Weiguo Liu [a, b], Hongxuan Lu [a], Chuanlun Zhang [c]

[a] State Key Laboratory of Loess and Quaternary Geology, Institute of Earth Environment, Chinese Academy of Sciences, Xi'an 710061, China
[b] School of Human Settlement and Civil Engineering, Xi'an Jiaotong University, Xi'an 710049, China
[c] State Key Laboratory of Marine Geology, Tongji University, Shanghai 200092, China

ARTICLE INFO

Article history:
Received 30 August 2016
Received in revised form
6 November 2016
Accepted 9 November 2016
Available online 12 January 2017

Keywords:
GDGTs
BIT
$R_{i/b}$
Degradation
Chinese Loess Plateau

ABSTRACT

Two indices based on the relative abundance of isoprenoid glycerol dialkyl glycerol tetraethers (isoGDGTs) to branched GDGTs (brGDGTs), i.e., the branched and isoprenoid tetraether (BIT) index and the ratio of isoGDGTs to brGDGTs ($R_{i/b}$) index, have recently been proposed as promising proxies for tracing humidity variations in terrestrial soil deposits. However, the applicability of these proxies in loess–paleosol sequences (LPSs) remains unclear on the Chinese Loess Plateau (CLP). In this study, we analyzed BIT, $R_{i/b}$ and concentrations of related GDGTs in 37 surface soil samples on the CLP. The results showed that the concentrations of brGDGTs correlate positively (strongly or moderately) with soil water content (SWC; $r = 0.74$) and mean annual precipitation (MAP; $r = 0.58$), while the concentrations of isoGDGTs correlate negatively (but generally weakly) with SWC ($r = -0.31$) and MAP ($r = -0.45$), and consequently, there is a positive relationship between BIT and moisture, and a negative relationship between $R_{i/b}$ and moisture. Despite the sensitivity of BIT and $R_{i/b}$ to moisture variations on the modern CLP, the published records in 3 LPSs consistently show an increasing trend in BIT and a decreasing trend in $R_{i/b}$ with age, which are insensitive to past changes in Asian summer monsoon intensity. This fact suggests that the two indices might not be sensitive recorders of past hydrological changes in LPSs on the CLP. Further analysis of GDGT concentrations in the Lantian LPS showed strong and negative exponential relationships between isoGDGT concentrations and age but weak relationships between brGDGT concentrations and age, possibly indicating faster degradation of isoGDGTs vs. brGDGTs in the LPSs. The preferential degradation of isoGDGTs vs. brGDGTs may potentially bias the BIT and $R_{i/b}$ indices towards higher and lower values, respectively, and thus might be at least partly responsible for the insensitivity of the two proxies for paleohydrologicial reconstructions in LPSs on the CLP. However, it should be noted that the preferential degradation of isoGDGTs vs. brGDGTs cannot affect other paleoproxies which are based only on isoGDGTs or brGDGTs, such as the TEX_{86} and MBT′/CBT indices.

1. Introduction

Glycerol-based alkyl ether lipids occurred ubiquitously in a wide range of environments such as oceans, lakes and soils (e.g. Liu et al., 2012; Schouten et al., 2013; Heyng et al., 2015; Yamamoto et al., 2016). Among these biomarker lipids, two types of tetraethers, the so-called isoprenoid glycerol dialkyl glycerol tetraethers (isoGDGTs) and branched GDGTs (brGDGTs) (Fig. 1), which are produced by archaea and bacteria, respectively (Schouten et al., 2013), are most commonly detected. About 10 years ago, Weijers et al. (2007) observed significant correlations between the distributions of brGDGTs and mean annual air temperature (MAT) and soil pH based upon an extensive survey of more than 130 natural soil samples globally distributed. Since then, the potential use of brGDGTs as paleoproxies for continental temperature and pH variations has been increasingly investigated (e.g. Peterse et al., 2012; De Jonge et al., 2014; Yang et al., 2014a; Zheng et al., 2016).

Along with the springing up of studies on brGDGTs-based temperature and pH proxies in modern soils, some researchers also noticed isoGDGTs and found that the relative distributions of

* Corresponding author.
E-mail address: wanghy@ieecas.cn (H. Wang).

http://dx.doi.org/10.1016/j.quaint.2016.11.004
1040-6182/

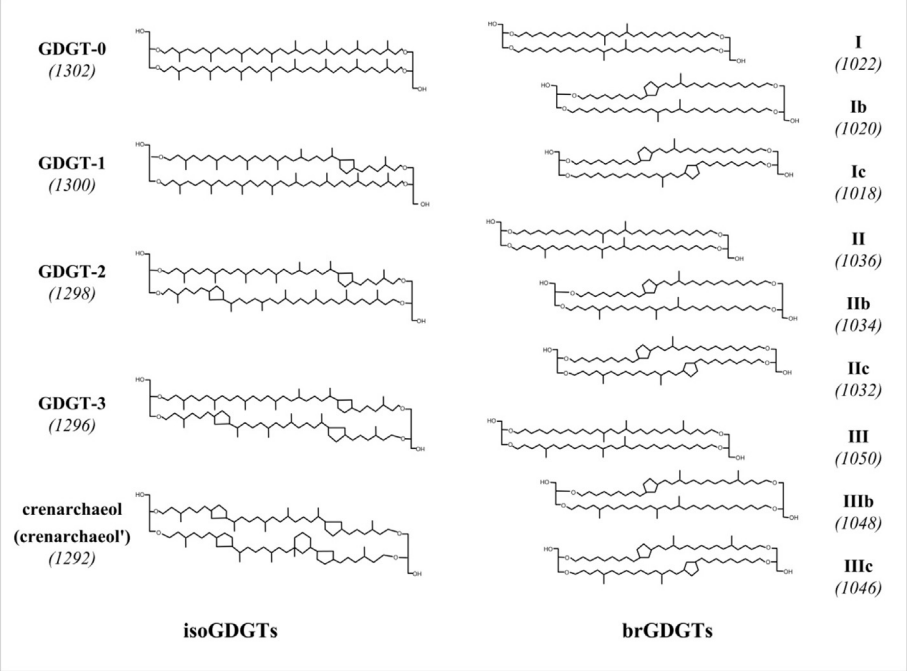

Fig. 1. Chemical structures of iso- and brGDGTs discussed in the text and their $[M+H]^+$ values.

the two types of GDGTs (isoGDGTs vs. brGDGTs) are sensitive to variations in moisture conditions (Xie et al., 2012; Dirghangi et al., 2013; Wang et al., 2013). By the study of 54 modern Chinese soil samples, Xie et al. (2012) found that the ratio of isoGDGTs to brGDGTs, expressed as the $R_{i/b}$ index, showed a sharp increase when soil pH is > 7.5 or mean annual precipitation (MAP) is < 600 mm, and therefore, the $R_{i/b}$ index was proposed as a proxy for alkaline conditions particularly induced by enhanced aridity. Subsequently, the indication of $R_{i/b}$ and BIT for aridity was validated by an extended dataset of more than 100 surface soil samples across a large climatic gradient of China (Yang et al., 2014a), the independent datasets from two soil transects in the USA (Dirghangi et al., 2013), two marsh-soil transects surrounding Lake Qinghai, China (Wang et al., 2013), and 41 surface soil samples from around Lake Qinghai and Qaidam Basin on the Northeastern Qinghai-Tibetan Plateau (NE QTP), China (Sun et al., 2016). Moreover, by the study of soil samples collected across two environmental transects in the USA (a dry, western transect and a wet, east coast transect) with distinct precipitation characteristics, Dirghangi et al. (2013) observed that the branched and isoprenoid tetraether (BIT) index (defined by Hopmans et al., 2004), which quantifies the relative abundances of crenarchaeol and three major bGDGTs (I+II+III), showed a reasonably good relationship with MAP. Meanwhile, a significant positive correlation between the BIT index and soil water content (SWC) was established along two transects extending from the lake shore marsh to upland soils on the NE QTP (Wang et al., 2013). Therefore, the BIT index which was originally proposed as a proxy for estimating the relative amounts of terrestrial organic matter input in marine and lake sediments (Hopmans et al., 2004) is also promising for tracing moisture variation in terrestrial soil deposits (Wang et al., 2013). The positive relation between BIT and moisture (MAP or SWC) was also confirmed by surface soil investigations across a large climatic gradient of China (Yang et al., 2014a) and on the NE QTP (Sun et al., 2016).

The sensitivity of the $R_{i/b}$ and BIT indices to moisture variations in modern environments led to the application of them as paleohydrological proxies in ancient deposits. Xie et al. (2012) suggest that the elevated $R_{i/b}$ values at ca. 9 Ma in a fluvio-lacustrine section in the Zhada basin of the southwestern QTP possibly indicated severe drought event associated with significant uplift of the QTP in the Late Miocene. In the Weinan loess–paleosol sequence (LPS) on the Chinese Loess Plateau (CLP), the significant increase of the $R_{i/b}$ ratio from 0.11 at the Holocene Thermal Maximum to 1.26 at the late Holocene was explained as enhanced aridity in late Holocene (Yang et al., 2014a). In the Crvenka LPS (Zech et al., 2013) and Surduk LPS (Schreuder et al., 2016), Northern Serbia, the higher BIT values in the MIS 1, 3 (and 5) paleosols, and lower BIT values in the MIS 2 (and 6) loess seem to indicate humid glacials and arid interglacials in Southeast Europe.

The continuous and long LPSs on the CLP are important continental archives of past climate change (Liu, 1985; Liu and Ding, 1998; An, 2000; Zhang et al., 2010; Cai et al., 2013; Sun and Feng, 2015; Liu and Liu, in press). Recently, the brGDGT-based palaeotemperature proxies have been applied to LPSs from Mangshan (Peterse et al., 2011, 2014), Lantian (Gao et al., 2012; Lu et al., 2016), Yuanbao (Jia et al., 2013), and Weinan (Yang et al., 2014a,b). The $R_{i/b}$ and BIT indices, if validated, may provide additional approaches for paleohydrological reconstruction in LPSs on the CLP. This is of particular interest in view of the advantage that the two indices can be obtained along with the brGDGT-based temperature and pH proxies in a single GDGT analysis. However, in the Yuanbao LPS, Jia et al. (2013) pointed out that the decreasing trend of BIT (or increasing trend of $R_{i/b}$) since the early Holocene may be due to enhanced archaea production relative to that of brGDGT-producing bacteria, and other possibilities, such as preferential degradation of isoGDGTs or upward increase in living archaea relative to bacteria in the paleosol profile is also likely. Hence, despite that the BIT and $R_{i/b}$ indices are sensitive to moisture variations in a wide range of modern soil conditions (Xie et al., 2012; Dirghangi et al., 2013; Wang et al., 2013; Yang et al., 2014a; Sun et al., 2016), the applicability of two paleohydrological proxies remains unclear on the CLP.

In this study, we first analyze BIT, $R_{i/b}$ and concentrations of related GDGTs in 37 surface soils specifically on the CLP to

investigate their modern relations with moisture conditions. Then we synthesize published BIT and $R_{i/b}$ records in 3 LPSs (Jia et al., 2013; Yang et al., 2014b; Lu et al., 2016) to see their ancient performance on the CLP. Finally, we analyze the records of isoGDGT concentrations in the Lantian LPS and combined it with those of brGDGT concentrations (Lu et al., 2016) to investigate the degradation of the two types of GDGTs and its potential effect on BIT and $R_{i/b}$. Our ultimate goal was to systematically assess the applicability of the two indices as paleohydrological proxies in LPSs on the CLP.

2. Materials and methods

2.1. Geological setting and sampling

The CLP is the largest region of wind-blown dust (i.e. loess) deposits in the world. The cyclic alternation of loess and paleosol which have accumulated at least over the past 2.6 Ma (Liu, 1985; Liu and Ding, 1998) provides highly visible records of regional climate variations due to changes in monsoon intensity on glacial-interglacial time scales (An, 2000; Porter, 2001). The present-day climate on the CLP is temperate semiarid and subhumid monsoon climate, with precipitation occurring mostly during the summer months (June to August; accounts for approximately 68–87% of the total annual precipitation) and exhibiting a clearly decreasing trend in mean annual values northwestwards (Ding, 1994; Liu et al., 2005a). Resulting from increasing dryness, the vegetation progressively becomes sparser and less dense from southeast to northwest (Liu et al., 2005b).

In late September 2012, 19 surface (0–5 cm) soil samples along a south-north transect and 18 along a southeast-northwest transect were collected at 12 county/town sites in natural grassland (or grassland in restoration for over 10 years) on the CLP (Fig. 2). For each site, 2–5 samples were collected at locations tens to hundreds of meters apart and each sample represents a mixture of three subsamples collected randomly at one location. The distributions of brGDGTs, SWC and MAP values for the 37 surface soil samples have been reported in Wang et al. (2014). The details of the samples are provided in Table 1. We also sampled loess samples along the LPS at the Lantian County (109°12′E, 34°12′N) that lies on the southern CLP (Fig. 2). A total of 90 samples were taken at 20 cm intervals, representing an average sampling resolution of ca. 1.6 ka based on the age model of Gao et al. (2012). The BIT, $R_{i/b}$ and brGDGTs data for the Lantian LPS has been reported in Lu et al. (2016).

2.2. Analysis of GDGTs

The extraction procedure and analytical methods has been described in Wang et al. (2014) and Lu et al. (2016), respectively. Briefly, approximately 30 g freeze dried and homogenized samples for surface soils and 10 g homogenized samples for LPS were extracted 4 times with dichloromethane (DCM):methanol (9:1, v/v) using an accelerated solvent extractor (ASE 350, Dionex) at 100 °C

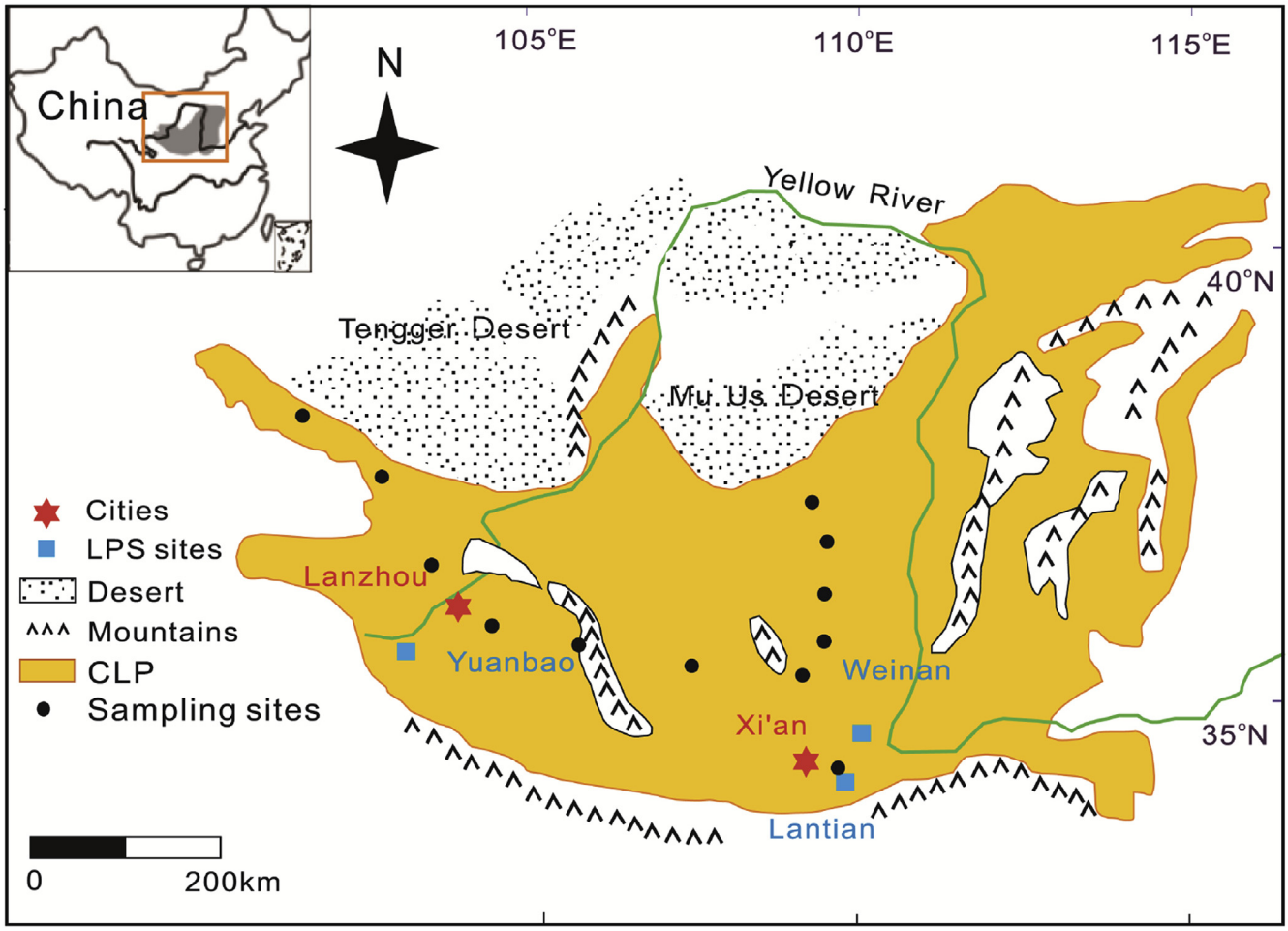

Fig. 2. Sketch map of the CLP and its surroundings (modified from Zhao et al., 2014) showing the 12 sampling sites of surface soil samples in this work (For each site, 2–5 samples were collected at locations tens to hundreds of meters apart). The sites of three LPS sections, i.e., Yuanbao (Jia et al., 2013), Weinan (Yang et al., 2014b) and Lantian (Lu et al., 2016 and this study) are also indicated.

Table 1
Overview of the sampling sites, environmental variables (SWC and MAP), the BIT and $R_{i/b}$ indices and the concentrations of related GDGTs for 37 surface soil samples on the CLP.

No.	ID	Latitude (N)	Longitude (E)	SWC (%)	MAP (mm)	GDGT concentration (ng g^{-1})				BIT	$R_{i/b}$
						isoGDGTs	brGDGTs	I+II+III	Cren		
1	WLPS-1	35°21′21.894″	107°41′6.163″	16.3	575	6.6	11.7	9.6	3.7	0.72	0.57
2	WLPS-2	35°21′16.357″	107°41′1.778″	13.8	575	4.0	5.6	4.3	2.2	0.66	0.71
3	WLPS-3	35°21′16.573″	107°41′1.622″	15.7	575	4.3	5.6	4.0	1.8	0.69	0.76
4	WLPS-4	35°35′57.574″	106°01′2.898″	6.9	492	6.6	6.7	5.9	3.3	0.64	0.99
5	WLPS-5	35°35′58.297″	106°00′59.728″	10.9	492	4.2	3.3	2.9	2.6	0.53	1.29
6	WLPS-6	35°35′57.380″	106°00′59.603″	6.4	492	5.6	5.3	4.5	3.1	0.59	1.06
7	WLPS-7	35°47′9.466″	104°18′13.231″	15.9	372	5.1	4.3	3.7	2.9	0.56	1.20
8	WLPS-8	35°47′11.043″	104°18′12.397″	17.1	372	13.8	9.6	8.6	8.3	0.51	1.43
9	WLPS-9	35°47′12.696″	104°18′11.940″	16.2	372	4.0	2.4	2.2	1.9	0.53	1.69
10	WLPS-10	36°29′26.033″	103°23′58.472″	13.3	284	7.9	10.2	9.7	4.9	0.66	0.78
11	WLPS-11	36°29′27.352″	103°23′56.563″	12.7	284	7.5	13.8	12.8	4.5	0.74	0.54
12	WLPS-12	36°29′26.116″	103°23′57.509″	12.0	284	4.4	6.2	5.8	2.5	0.70	0.71
13	WLPS-13	37°30′0.853″	102°52′34.941″	2.8	352	10.0	2.4	2.3	4.1	0.36	4.15
14	WLPS-14	37°30′0.263″	102°52′31.514″	6.1	352	16.2	2.7	2.6	6.1	0.30	6.04
15	WLPS-15	37°29′56.483″	102°52′42.411″	2.7	352	8.2	1.9	1.8	2.8	0.38	4.41
16	WLPS-16	38°15′8.88″	101°59′16.747″	6.5	212	7.2	3.7	3.5	3.9	0.47	1.94
17	WLPS-17	38°15′8.463″	101°59′16.212″	13.7	212	25.1	6.1	5.8	13.7	0.30	4.12
18	WLPS-18	38°15′16.131″	101°59′6.22″	3.9	212	22.9	8.7	8.4	12.7	0.40	2.64
19	WLPS-79	37°04′38.372″	109°04′55.748″	14.2	507	5.1	8.3	6.9	2.1	0.76	0.61
20	WLPS-80	37°04′38.946″	109°04′55.026″	15.6	507	3.5	4.7	4.0	1.8	0.69	0.74
21	WLPS-81	37°04′38.846″	109°04′54.684″	12.2	507	2.0	4.7	4.0	1.1	0.79	0.42
22	WLPS-82	36°41′22.886″	109°24′57.159″	16.8	515	4.1	8.6	6.8	2.4	0.74	0.47
23	WLPS-83	36°41′22.605″	109°24′56.584″	19.1	515	1.7	3.5	3.0	1.0	0.75	0.49
24	WLPS-84	36°41′24.131″	109°24′57.897″	20.2	515	4.1	8.9	7.3	2.3	0.76	0.46
25	WLPS-85	36°14′09.683″	109°22′38.914″	16.9	531	3.6	6.0	4.7	1.8	0.72	0.60
26	WLPS-86	36°14′09.452″	109°22′37.544″	17.8	531	3.9	6.2	5.1	1.9	0.73	0.63
27	WLPS-87	36°14′10.393″	109°22′39.430″	17.8	531	3.2	6.2	4.9	1.6	0.75	0.52
28	WLPS-88	35°42′42.520″	109°25′02.876″	20.3	592	6.6	15.3	11.2	4.1	0.73	0.43
29	WLPS-89	35°42′42.495″	109°25′02.568″	18.6	592	7.8	11.9	9.5	4.6	0.68	0.66
30	WLPS-90	35°42′30.762″	109°25′11.366″	19.9	592	4.7	13.6	10.0	2.7	0.79	0.35
31	WLPS-91	35°23′20.902″	109°07′58.947″	24.1	676	5.8	42.8	30.0	3.1	0.91	0.14
32	WLPS-92	35°23′20.902″	109°07′58.947″	28.0	676	7.3	68.3	43.1	4.3	0.91	0.11
33	WLPS-93	34°14′27.333″	109°07′27.652″	21.5	636	7.3	14.4	11.5	4.4	0.72	0.50
34	WLPS-94	34°14′30.420″	109°07′30.744″	23.6	636	4.0	16.7	12.2	2.4	0.84	0.24
35	WLPS-95	34°14′22.393″	109°07′25.504″	22.7	636	6.3	23.7	16.6	4.1	0.80	0.27
36	WLPS-96	34°14′22.705″	109°07′25.021″	21.1	636	7.6	21.8	15.5	5.0	0.76	0.35
37	WLPS-97	34°14′19.807″	109°07′24.699″	20.8	636	7.6	36.4	19.8	5.1	0.80	0.21

and 1500 psi. The total extract (TLE) was dried under N_2 in a water bath and half of the TLE for surface soils and the polar fractions for LPS samples were filtered over a 0.45 μm PTFE filter by hexane/isopropanol (99:1 v/v). Analysis of GDGTs was performed on high performance liquid chromatography/atmospheric pressure chemical ionization-mass spectrometry (HPLC-APCI-MS). For surface soil samples, separation of GDGTs was achieved on an Alltech Prevail Cyano Column (150 mm × 2.1 mm, 3 μm) at a flow rate of 0.2 ml/min. For Lantian LPS samples, Separation of GDGTs was obtained with two coupled Inertsil SIL-100A silica columns (each 250 mm × 4.6 mm, 3 μm), with total flow rate of pump A and pump B maintained at 0.6 ml/min. Selective ion monitoring (SIM) mode was used to detect the $[M+H]^+$ (mass to charge ratio of protonated molecular ion) of isoGDGTs and brGDGTs. Quantification of each GDGT was achieved by calculating the peak area of $[M+H]^+$ in the chromatogram and comparing it with that of the C_{46} internal standard (IS, Huguet et al., 2006), based on the assumption that the ionization efficiency for GDGTs and the IS was identical.

The BIT index was calculated following Hopmans et al. (2004):

$$BIT = (I + II + III)/(I + II + III + crenarchaeol) \quad (1)$$

The $R_{i/b}$ index was calculated according to Xie et al. (2012):

$$R_{i/b} = \sum isoGDGTs \Big/ \sum brGDGTs \quad (2)$$

3. Results and discussion

3.1. Response of iso- and brGDGTs to moisture conditions on the modern CLP

An ideal way to quantify the moisture conditions of growth environment for the GDGT producers in soils is to measure the variation of year-round SWC. However, the year-round SWC is currently not available for the 37 samples investigated here. In previous studies both SWC at the time of sampling and MAP have been used to investigate the hydrological effect on GDGT distributions (e.g. Peterse et al., 2012; Dirghangi et al., 2013; Wang et al., 2013; Yang et al., 2014a; Dang et al., 2016), but both of them have advantages and pitfalls compared with each other. For example, on a large spatial scale, MAP values would be more representative for the mean soil moisture conditions than the instantaneous SWC values which might be susceptible to local rainfall, when continuous local soil moisture observation data was not available (Wang et al., 2014). However, on a smaller spatial scale, soil moisture for samples at sites with identical MAP might still vary significantly due to differences in soil texture, topography, water table depth, evapotranspiration, and vegetation, etc (Crave and Gascuel-Odoux, 1997; Gómez-Plaza et al., 2001; Wang et al., 2013; Dang et al., 2016). In such cases, the SWC values at the sampling time might be more suitable for distinguishing differences in soil moisture than the regionally-averaged MAP values that were measured by weather

stations. Accordingly, they were both used to roughly represent moisture conditions for our samples in this study, and we believe that similar GDGT-SWC and GDGT-MAP relations may actually reflect the effect of moisture conditions on GDGTs.

In surface soil samples on the modern CLP, the concentrations of total brGDGTs or I+II+III correlate positively with SWC and MAP (r = 0.74, 0.58, 0.69, 0.50 for brGDGTs vs. SWC, brGDGTs vs. MAP, I+II+III vs. SWC, I+II+III vs. MAP, respectively), while the concentrations of total isoGDGTs or crenarchaeol correlate negatively with SWC and MAP (r = −0.31, −0.45, −0.16, −0.37 for isoGDGTs vs. SWC, isoGDGTs vs. MAP, crenarchaeol vs. SWC, crenarchaeol vs. MAP, respectively) (Fig. 3a–d). Consequently, the BIT index which represents the relative abundance of I+II+III to crenarchaeol shows a positive relationship with SWC or MAP (r = 0.78 and 0.76, respectively; Fig. 3e and f), and the $R_{i/b}$ index which represents the relative abundance of isoGDGTs to brGDGTs shows a negative relationship with SWC or MAP (r = −0.84 and −0.78, respectively; Fig. 3e and f). The relationships between BIT and moisture and

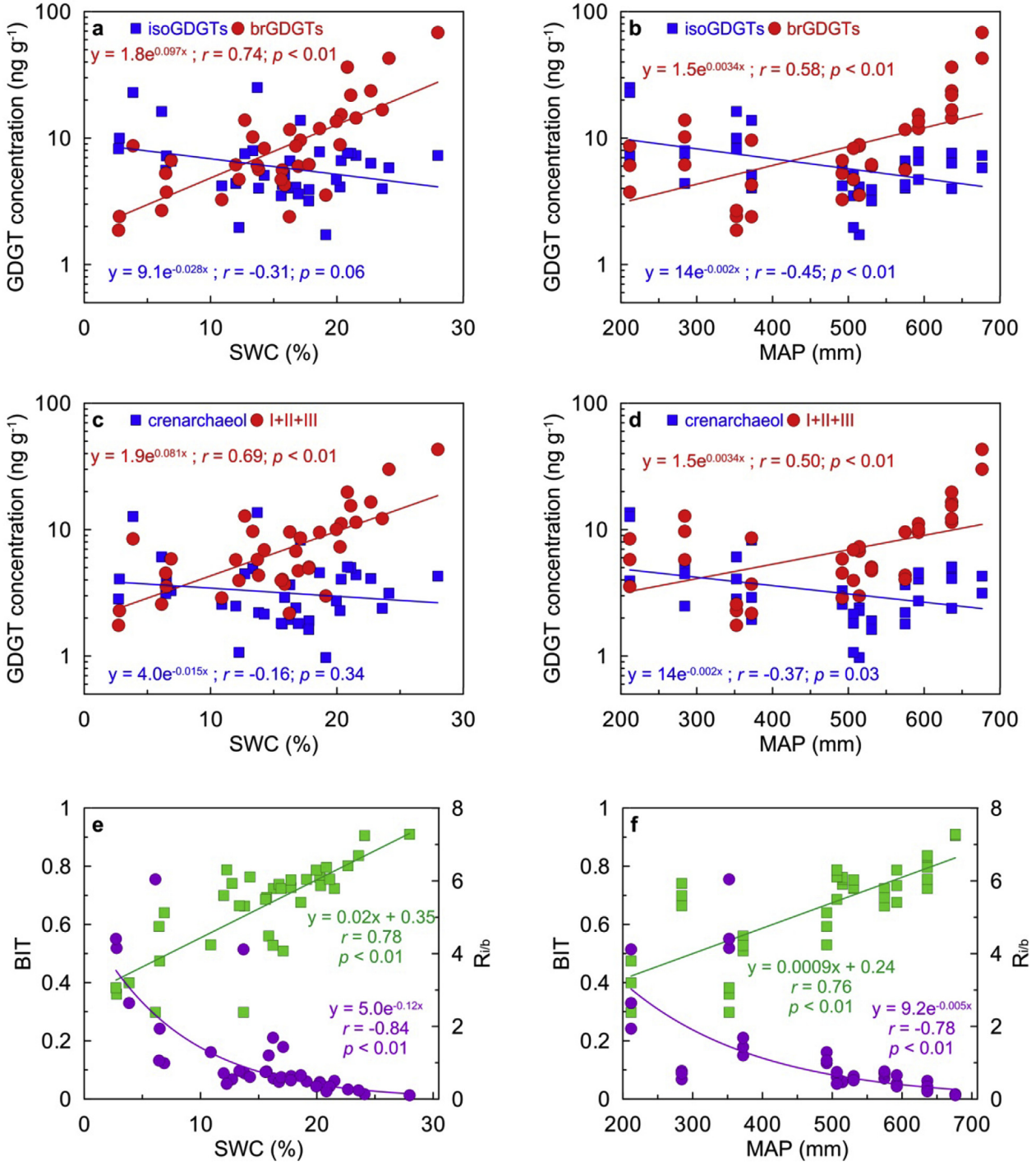

Fig. 3. Correlations between GDGTs and moisture conditions in surface soil samples on the CLP. (a) Concentrations of $R_{i/b}$-related GDGTs (iso- or brGDGTs) vs. SWC. (b) Concentrations of $R_{i/b}$-related GDGTs (iso- or brGDGTs) vs. MAP. (c) Concentrations of BIT-related GDGTs (crenarchaeol or I+II+III) vs. SWC. (d) Concentrations of BIT-related GDGTs (crenarchaeol or I+II+III) vs. MAP. (e) BIT (or $R_{i/b}$) vs. SWC. (f) BIT (or $R_{i/b}$) vs. MAP. In (e) and (f), squares indicate BIT while circles indicate $R_{i/b}$.

between $R_{i/b}$ and moisture on the modern CLP are in accord with the recent investigations of modern soils in China and North America (Xie et al., 2012; Dirghangi et al., 2013; Wang et al., 2013; Sun et al., 2016), further validating the moisture control on the two indices that represent the relative abundance of the two types of GDGTs.

The mechanism for the moisture–$R_{i/b}$ (BIT) relationship remains speculative. It might reflect a direct control of soil moisture, or some parameter(s) related to or regulated by soil moisture (e.g. O_2 concentration and TOC content), on the producers of brGDGTs and isoGDGTs (Wang et al., 2013; Sun et al., 2016). In addition, we should point out that, for our surface soil samples on the CLP, the correlations between brGDGTs (or I+II+III) concentration and moisture condition (expressed as MAP or SWC) are much stronger than those between isoGDGTs (crenarchaeol) concentration and moisture condition (Fig. 3a–d). This possibly indicates that soil moisture has a much stronger control on the activity of brGDGT-producing bacteria in this region.

3.2. Performance of BIT and $R_{i/b}$ in LPSs on the CLP

The good relationships between $R_{i/b}$ (BIT) and MAP (SWC) in surface soil samples suggest that these two indices are sensitive to soil moisture conditions on the modern CLP. However, whether or not they can be used as reliable paleohydrological proxies on the CLP remains to be tested by their performance in LPSs. Currently, there are 3 LPSs with published BIT and $R_{i/b}$ data, namely, the Yuanbao LPS (0.9–67.5 ka BP; Jia et al., 2013), the Weinan LPS (0.2–73.1 ka BP; Yang et al., 2014b), and the Lantian LPS (2.9–115.6 ka BP; Lu et al., 2016). The BIT, $R_{i/b}$, and magnetic susceptibility data of the 3 profiles are compiled in Fig. 4. The BIT records consistently show a decreasing trend towards the late Holocene, while the $R_{i/b}$ records consistently exhibit an increasing trend in the 3 LPSs (Fig. 4). Magnetic susceptibility is a traditional proxy for Asian monsoon precipitation in the LPSs, with higher magnetic susceptibility indicating stronger pedogenesis caused by enhanced summer monsoon intensity and vice versa (An et al., 1990; Maher et al., 1994). However, although the overall trends of the BIT and $R_{i/b}$ indices are both in agreement with the decreasing trend of magnetic susceptibility towards present, the variations in BIT and $R_{i/b}$ do not follow fluctuations of the magnetic susceptibility records for each LPS (Fig. 4). Further, the BIT ($R_{i/b}$) values are generally higher (lower) in L_1LL_1 than in its overlaying paleosol S_0, and similarly, BIT ($R_{i/b}$) values are generally higher (lower) in L_1LL_2 than in L_1LS_1 (Fig. 4). Based on the relationships between BIT ($R_{i/b}$) and moisture on the modern CLP, one might argue that loess (L_1LL_1 and L_1LL_2) may have formed under wetter conditions while paleosol (S_0) and weak paleosol (L_1LS_1) may have formed under drier conditions. This hypothesis is, however, in conflict with the widely accepted view concerning the formation of the loess and paleosol layers (Liu, 1985; An, 2000; Porter, 2001). Therefore, it seems that the BIT and $R_{i/b}$ indices based on GDGTs produced by soil microorganisms are unconvincing when being used to infer past climatic changes in LPSs on the CLP.

3.3. Degradation of GDGTs in LPSs on the CLP and impact on BIT and $R_{i/b}$

The redox condition is a key factor controlling the preservation of organic matters (e.g. Ding et al., 2014). LPSs on the CLP are generally deposited under oxidation condition (Liu et al., 2008), and therefore may have suffered from relatively strong degradation of organic matters, including GDGTs. Actually, despite that regional paleoclimate have varied significantly in glacial-interglacial cycles, we have observed strong and negative exponential relationships between the concentration of crenarchaeol and age ($r = 0.92$, $p < 0.01$), and between the concentration of isoGDGTs and age ($r = 0.86$, $p < 0.01$) for the Lantian LPS (Fig. 5), possibly suggesting considerable degradation of isoGDGTs. On the other hand, the negative exponential relationship between the concentration of I+II+II (or brGDGTs) and age is weaker ($r = 0.35$ for I+II+II and 0.33 for brGDGTs, $p < 0.01$), possibly indicating that brGDGTs are relatively resistant to diagenesis than isoGDGTs in LPSs. The preferential degradation of isoGDGTs in the LPS is consistent with previous field investigations in ancient marine sediments (Huguet et al., 2008) and modeling experiments (Ding et al., 2013). By analyzing GDGT concentrations across oxidation fronts in organic matter-rich turbidites from the Madeira Abyssal Plain, Huguet et al. (2008) observed that the degradation rate of crenarchaeol is 2-fold higher than that of brGDGTs upon long-term oxygen exposure. In

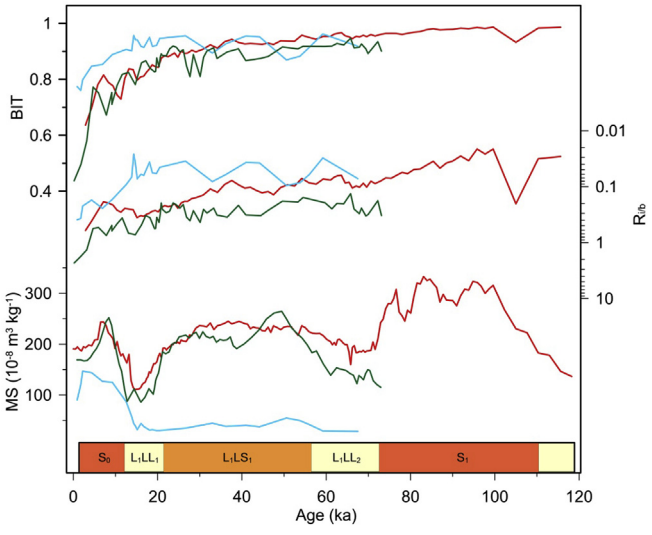

Fig. 4. The BIT, $R_{i/b}$ and magnetic susceptibility records of 3 LPSs on the CLP. The blue lines, green lines and red lines represent those for Yuanbao (Jia et al., 2013), Weinan (Yang et al., 2014b) and Lantian (Lu et al., 2016), respectively. (For interpretation of the references to colour in this figure legend, the reader is referred to the web version of this article.)

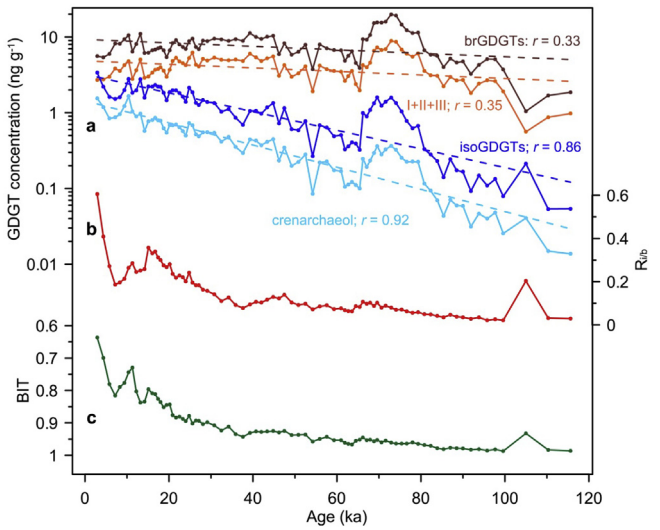

Fig. 5. Variations in GDGT concentrations and the BIT and $R_{i/b}$ indices in the Lantian LPS. (a) Concentrations of brGDGTs, I+II+III, isoGDGTs, and crenarchaeol. The dotted lines represent the regressions of GDGT concentrations vs. age. (b) the $R_{i/b}$ record (Lu et al., 2016). (c) the BIT record (Lu et al., 2016).

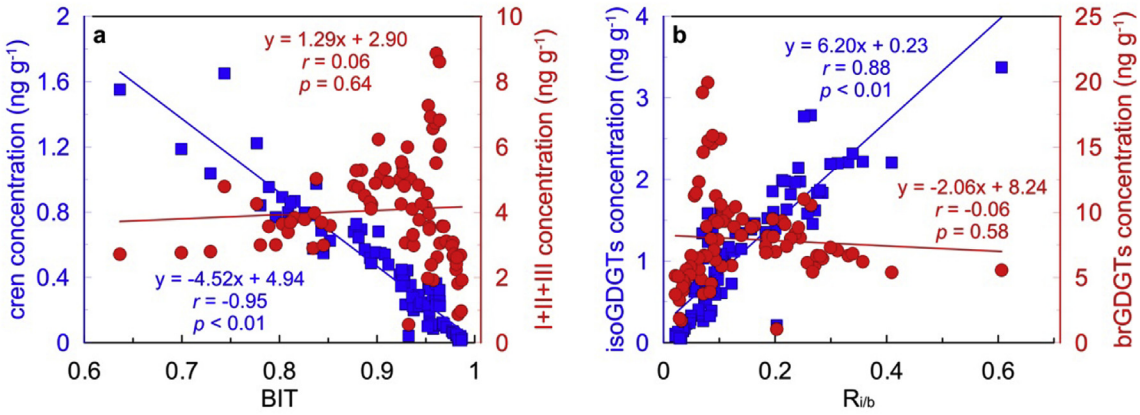

Fig. 6. Correlations between GDGT concentrations and GDGT indices in the Lantian LPS. (a) GDGT (squares indicate crenarchaeol while circles indicate I+II+III) concentrations vs. BIT. (b) GDGT (squares indicate isoGDGTs while circles indicate brGDGTs) concentrations vs. $R_{i/b}$.

a modeling experiment, Ding et al. (2013) also found that isoGDGTs are more easily degraded than brGDGTs for a modern soil sample after the oxidation by hydrogen peroxide.

The mechanism governing the differential degradation and preservation of these GDGTs in LPSs is still unclear. Huguet et al. (2008) attributed the selective preservation of brGDGTs in turbidites to matrix protection of soil-derived matter, rather than different degradation kinetics of isoGDGTs vs brGDGTs. For the surface soil sample in Ding et al. (2013) and loess-paleosol samples in this study, however, this mechanism is not applicable since both isoGDGTs and brGDGTs are produced by soil microorganisms. Regardless of the mechanism, the differential degradation of isoGDGTs vs. brGDGTs could potentially result in biased higher BIT values and lower $R_{i/b}$ values for ancient LPS deposits. It could also readily explain the prevailing increasing (decreasing) trend in BIT ($R_{i/b}$) with age in the LPSs (Fig. 4). Actually, in the Yuanbao LPS, Jia et al. (2013) have already speculated that the higher degradation rate of isoGDGTs is one possibility responsible for the decreasing trend of BIT and increasing trend of $R_{i/b}$ since the early Holocene.

The effect of preferential degradation of isoGDGTs on the BIT and $R_{i/b}$ indices is more evident if we compare the correlations between the two indices and GDGT concentrations for surface soils and the Lantian LPS. Based on the modern results for surface soil samples on the CLP, I+II+II and brGDGTs are more sensitive to soil moisture compared with crenarchaeol and isoGDGTs (Fig. 3), and consequently, the variations of BIT and $R_{i/b}$ are more dependent on the concentrations of I+II+II and brGDGTs, respectively. In the Lantian LPS, however, BIT and $R_{i/b}$ correlate much strongly with the concentrations of crenarchaeol ($r = -0.95$; $p < 0.01$) and isoGDGTs ($r = 0.88$; $p < 0.01$), respectively, while the correlations between BIT and I+II+II ($r = 0.06$; $p = 0.64$) and between $R_{i/b}$ and brGDGTs ($r = -0.06$; $p = 0.58$) are both quite weak (Fig. 6). Consequently, the increasing trend of BIT and decreasing trend of $R_{i/b}$ with age seem mainly reflect the decreases in concentrations of crenarchaeol and isoGDGTs (Fig. 5), respectively, which result from the increasing degradation effect with age, rather than variations in the concentrations of I+II+II and brGDGTs.

We should point out that the preferential degradation of isoGDGTs vs. brGDGTs cannot impact paleoproxies such as the TEX_{86} index, the cyclisation ratio of branched tetraethers (CBT), and the brGDGT-based temperature proxies, which are based only on one type of GDGTs (either isoGDGTs or brGDGTs) in LPSs on the CLP. Also, it seems that the effect of selective degradation within one type of GDGTs on paleoproxies is weak. For example, in the Mangshan (Peterse et al., 2011, 2014), Lantian (Gao et al., 2012; Lu et al., 2016), Yuanbao (Jia et al., 2013), and Weinan (Yang et al., 2014a,b) LPSs, the reconstructed temperature and hydrological records based on brGDGTs are consistent with variations in solar insolation and summer monsoon, respectively, suggesting that the degradation of GDGTs does probably not play a significant role on paleoproxies based on one type of GDGTs (either isoGDGTs or brGDGTs), possibly due to the similar chemical structures and thus similar degradation rates of compounds within one GDGT group.

4. Implications and conclusions

In surface soil samples on the modern CLP, the concentration of brGDGTs correlates positively (strongly or moderately) with SWC and MAP, while the concentration of isoGDGTs correlates negatively (but generally weakly) with SWC and MAP, resulting in a positive relationship between BIT and moisture, and a negative relationship between $R_{i/b}$ and moisture. This possibly supports a strong control of moisture on the community structure of GDGT-producing microorganisms in modern soils.

In the ancient deposits (i.e., LPSs) on the CLP, however, the BIT and $R_{i/b}$ records seems not sensitive to past changes in Asian summer monsoon intensity, and predominantly exhibit a decreasing (increasing) trend with age. This is possibly mainly due to the preferential degradation of isoGDGTs vs. brGDGTs, as indicated by strong and negative exponential relationships between isoGDGT concentrations and age but weak relationships between brGDGT concentrations and age. Hence, the BIT and $R_{i/b}$ indices might not be sensitive recorders of past hydrological changes in LPSs on the CLP. However, it should be noted that the preferential degradation effect can only bias BIT and $R_{i/b}$ towards higher and lower values, respectively, and therefore, significantly lower BIT and higher $R_{i/b}$ values compared with those in episodes both before and after are possibly still useful for indicating the occurrence of drought events in the LPSs. Moreover, the preferential degradation of isoGDGTs vs. brGDGTs cannot impact paleoproxies based on only one type of GDGTs.

Acknowledgements

The China Meteorological Data Sharing Service System is thanked for providing free climatic data. Two anonymous reviewers are thanked for their useful comments. This research was financially supported by the National Natural Science Foundation of China (41420104008), the National Basic Research Program of

China (2013CB955901), and the National Natural Science Foundation of China (41573005, 41602183).

References

An, Z., Liu, T., Lu, Y., Porter, S.C., Kukla, G., Wu, X., Hua, Y., 1990. The long-term paleomonsoon variation recorded by the loess-paleosol sequence in Central China. Quat. Int. 7, 91–95.

An, Z., 2000. The history and variability of the East Asian paleomonsoon climate. Quat. Sci. Rev. 19, 171–187.

Cai, M., Wei, M., Xu, D., Miao, Y., Wu, F., Pan, B., 2013. Vegetation and climate changes during three interglacial periods represented in the Luochuan loess-paleosol section, on the Chinese Loess Plateau. Quat. Int. 296, 131–140.

Crave, A., Gascuel-Odoux, C., 1997. The influence of topography on time and space distribution of soil surface water content. Hydrol. Process. 11, 203–210.

Dang, X., Yang, H., Naafs, B.D.A., Pancost, R.D., Xie, S., 2016. Evidence of moisture control on the methylation of branched glycerol dialkyl glycerol tetraethers in semi-arid and arid soils. Geochim. Cosmochim. Acta 189, 24–36.

De Jonge, C., Hopmans, E.C., Zell, C.I., Kim, J.-H., Schouten, S., Sinninghe Damsté, J.S., 2014. Occurrence and abundance of 6-methyl branched glycerol dialkyl glycerol tetraethers in soils: implications for palaeoclimate reconstruction. Geochim. Cosmochim. Acta 141, 97–112.

Ding, W., Yang, H., He, G., Xie, S., 2013. Effect of oxidative degradation by hydrogen peroxide on tetraethers based organic proxies. Quat. Sci. 33, 39–47.

Ding, X., Liu, G., Lu, X., Huang, Z., Sun, M., Chen, Z., Liuzhuang, X., 2014. The impact on organic matter preservation by the degree of oxidation and reduction and sedimentation rates of Erlian Basin. Nat. Gas. Geosci. 25 (6), 810–817.

Ding, Y., 1994. Monsoons over China. Kluwer Academics Publishers, Dordrecht.

Dirghangi, S.S., Pagani, M., Hren, M.T., Tipple, B.J., 2013. Distribution of glycerol dialkyl glycerol tetraethers in soils from two environmental transects in the USA. Org. Geochem. 59, 49–60.

Gao, L., Nie, J.S., Clemens, S., Liu, W.G., Sun, J.M., Zech, R., Huang, Y.S., 2012. The importance of solar insolation on the temperature variations for the past 110 kyr on the Chinese Loess Plateau. Palaeogeogr. Palaeoclimatol. Palaeoecol. 317, 128–133.

Gómez-Plaza, A., Martínez-Mena, M., Albaladejo, J., Castillo, V.M., 2001. Factors regulating spatial distribution of soil water content in small semiarid catchments. J. Hydrol. 253, 211–226.

Heyng, A.M., Mayr, C., Lücke, A., Moschen, R., Wissel, H., Striewski, B., 2015. Middle and Late Holocene paleotemperatures reconstructed from oxygen isotopes and GDGTs of sediments from Lake Pupuke, New Zealand. Quat. Int. 374, 3–14.

Hopmans, E.C., Weijers, J.W.H., Schefuss, E., Herfort, L., Sinninghe Damsté, J.S., Schouten, S., 2004. A novel proxy for terrestrial organic matter in sediments based on branched and isoprenoid tetraether lipids. Earth Planet. Sci. Lett. 224, 107–116.

Huguet, C., Hopmans, E.C., Febo-Ayala, W., Thompson, D.H., Sinninghe Damsté, J.S., Schouten, S., 2006. An improved method to determine the absolute abundance of glyceroldibiphytanyl glycerol tetraether lipids. Org. Geochem. 37, 1036–1041.

Huguet, C., de Lange, G.J., Gustafsson, Ö., Middelburg, J.J., Sinninghe Damsté, J.S., Schouten, S., 2008. Selective preservation of soil organic matter in oxidized marine sediments (Madeira Abyssal Plain). Geochim. Cosmochim. Acta 72, 6061–6068.

Jia, G.D., Rao, Z.G., Zhang, J., Li, Z.Y., Chen, F.H., 2013. Tetraether biomarker records from a loess-paleosol sequence in the western Chinese Loess Plateau. Front. Microbiol. 4 http://dx.doi.org/10.3389/fmicb.2013.0019.

Liu, J., Liu, W., (in press). Soil nitrogen isotopic composition of the Xifeng loess-paleosol sequence and its potential for use as a paleoenvironmental proxy. Quat. Int. http://dx.doi.org/10.1016/j.quaint.2016.04.018.

Liu, T., 1985. Loess and the Environment. China Ocean Press, Beijing.

Liu, T., Ding, Z., 1998. Chinese loess and the paleomonsoon. Annu. Rev. Earth Planet. Sci. 26, 111–145.

Liu, W., Feng, X., Ning, Y., Zhang, Q., Cao, Y., An, Z., 2005a. $\delta^{13}C$ variation of C3 and C4 plants across an Asian monsoon rainfall gradient in arid northwestern China. Glob. Change Biol. 11, 1094–1100.

Liu, W., Ning, Y., An, Z., Wu, Z., Lu, H., Cao, Y., 2005b. Carbon isotopic composition of modern soil and paleosol as a response to vegetation change on the Chinese Loess Plateau. Sci. China Ser. D Earth Sci. 48, 93–99.

Liu, X., Liu, T., Paul, H., Xia, D., Jiri, C., Wang, G., 2008. Two pedogenic models for paleoclimatic records of magnetic susceptibility from Chinese and Siberian loess. Sci. China Ser. D Earth Sci. 51 (2), 284–293.

Liu, X.-L., Summons, R.E., Hinrichs, K.-U., 2012. Extending the known range of glycerol ether lipids in the environment: structural assignments based on tandem mass spectral fragmentation patterns. Rapid Commun. Mass Spectrom. 26, 2295–2302.

Lu, H., Liu, W., Wang, H., Wang, Z., 2016. Variation in 6-methyl branched glycerol dialkyl glycerol tetraethers in Lantian loess–paleosol sequence and effect on paleotemperature reconstruction. Org. Geochem. 100, 10–17.

Maher, B.A., Thompson, R., Zhou, L.P., 1994. Spatial and temporal reconstructions of changes in the Asian palaeomonsoon: a new mineral magnetic approach. Earth Planet. Sci. Lett. 125, 461–471.

Peterse, F., Prins, M.A., Beets, C.J., Troelstra, S.R., Zheng, H.B., Gu, Z.Y., Schouten, S., Sinninghe Damsté, J.S., 2011. Decoupled warming and monsoon precipitation in East Asia over the last deglaciation. Earth Planet. Sci. Lett. 301, 256–264.

Peterse, F., van der Meer, J., Schouten, S., Weijers, J.W.H., Fierer, N., Jackson, R.B., Kim, J.H., Sinninghe Damsté, J.S., 2012. Revised calibration of the MBT–CBT paleotemperature proxy based on branched tetraether membrane lipids in surface soils. Geochim. Cosmochim. Acta 96, 215–229.

Peterse, F., Martinez-Garcia, A., Zhou, B., Beets, C.J., Prins, M.A., Zheng, H.B., Eglinton, T.I., 2014. Molecular records of continental air temperature and monsoon precipitation variability in East Asia spanning the past 130,000 years. Quat. Sci. Rev. 83, 76–82.

Porter, S.C., 2001. Chinese loess record of monsoon climate during the last glacial–interglacial cycle. Earth Sci. Rev. 54, 115–128.

Schouten, S., Hopmans, E.C., Sinninghe Damsté, J.S., 2013. The organic geochemistry of glycerol dialkyl glycerol tetraether lipids: a review. Org. Geochem. 54, 19–61.

Schreuder, L.T., Beets, C.J., Prins, M.A., Hatté, C., Peterse, F., 2016. Late Pleistocene climate evolution in Southeastern Europe recorded by soil bacterial membrane lipids in Serbian loess. Palaeogeogr. Palaeoclimatol. Palaeoecol. 449, 141–148.

Sun, A., Feng, Z., 2015. Climatic changes in the western part of the Chinese Loess Plateau during the Last Deglacial and the Holocene: a synthesis of pollen records. Quat. Int. 372, 130–141.

Sun, C., Zhang, C., Li, F., Wang, H., Liu, W., 2016. Distribution of branched glycerol dialkyl glycerol tetraethers in soils on the Northeastern Qinghai-Tibetan Plateau and possible production by nitrite-reducing bacteria. Sci. China Earth Sci. 59, 1834–1846.

Wang, H., Liu, W., Zhang, C.L., Liu, Z., He, Y., 2013. Branched and isoprenoid tetraether (BIT) index traces water content along two marsh-soil transects surrounding Lake Qinghai: implications for paleo-humidity variation. Org. Geochem. 59, 75–81.

Wang, H., Liu, W., Zhang, C.L., 2014. Dependence of the cyclization of branched tetraethers on soil moisture in alkaline soils from arid–subhumid China: implications for palaeorainfall reconstructions on the Chinese Loess Plateau. Biogeosciences 11, 6755–6768.

Weijers, J.W.H., Schouten, S., van den Donker, J.C., Hopmans, E.C., Sinninghe Damsté, J.S., 2007. Environmental controls on bacterial tetraether membrane lipid distribution in soils. Geochim. Cosmochim. Acta 71, 703–713.

Xie, S., Pancost, R.D., Chen, L., Evershed, R.P., Yang, H., Zhang, K., 2012. Microbial lipid records of highly alkaline deposits and enhanced aridity associated with significant uplift of the Tibetan Plateau in the Late Miocene. Geology 40, 291–294.

Yamamoto, Y., Ajioka, T., Yamamoto, M., 2016. Climate reconstruction based on GDGT-based proxies in a paleosol sequence in Japan: postdepositional effect on the estimation of air temperature. Quat. Int. 397, 380–391.

Yang, H., Pancost, R.D., Dang, X., Zhou, X., Evershed, R.P., Xiao, G., Tang, C., Gao, L., Guo, Z., Xie, S., 2014a. Correlations between microbial tetraether lipids and environmental variables in Chinese soils: optimizing the paleo-reconstructions in semi-arid and arid regions. Geochim. Cosmochim. Acta 126, 49–69.

Yang, H., Pancost, R.D., Tang, C., Ding, W., Dang, X., Xie, S., 2014b. Distributions of isoprenoid and branched glycerol dialkanol diethers in Chinese surface soils and a loess–paleosol sequence: implications for the degradation of tetraether lipids. Org. Geochem. 66, 70–79.

Zech, R., Zech, M., Marković, S., Hambach, U., Huang, Y., 2013. Humid glacials, arid interglacials? Critical thoughts on pedogenesis and paleoclimate based on multi-proxy analyses of the loess–paleosol sequence Crvenka, Northern Serbia. Palaeogeogr. Palaeoclimatol. Palaeoecol. 387, 165–175.

Zhang, P., Liu, W., Qiang, X., Zhou, W., Wu, Z., Song, S., 2010. A test of stable carbon isotope record characteristics of phreatic and outcrop profiles. Quat. Int. 227, 75–80.

Zhao, H., Qiang, X., Sun, Y., 2014. Apparent timing and duration of the Matuyama-Brunhes geomagnetic reversal in Chinese loess. Geochem. Geophys. Geosyst. 15, 4468–4480.

Zheng, F., Zhang, C.L., Chen, Y., Li, F., Ma, C., Pu, Y., Zhu, Y., Wang, Y., Liu, W., 2016. Branched tetraether lipids in Chinese soils: evaluating the fidelity of MBT/CBT proxies as paleoenvironmental proxies. Sci. China Earth Sci. 59, 1353–1367.